LA-UR-17-23948
Approved for public release; distribution is unlimited.

Title: Trak Investigation of Focusing Electrode Geometries for the DARHT Axis-I Diode

Author(s): Kallas, Nicholas Dimitrious

Intended for: University and internal

Issued: 2017-05-15

Trak Investigation of Focusing Electrode Geometries for the DARHT Axis-I Diode

Nick Kallas

Los Alamos National Lab

Abstract: An investigation was carried out on the effects of different cathode shroud geometries of the DARHT Axis-1 diode using the Trak ray tracing software. Pierce angles of 20, 30, 45, 60, and 67.5 degrees were investigated [1]. For each geometry the current density with respect to radial position will be presented as it evolves in the longitudinal direction. In addition the emittances for each geometry are compared and this information is used to determine the optimal geometry from the selected angles. These results are compared to the baseline geometry currently employed at DARHT of a simple 2.5mm recessed velvet cathode. Of the selected angles it was found that 45 degrees produced the lowest normalized emittance value, whereas 60 degrees produced the most uniform current density profile at 1cm away from the emission surface. For the purpose of this investigation the effects of the bucking coil and solenoid around the hollow anode of the DARHT Axis I injector are neglected [2].

Introduction:

High current electron beams generated by dielectric fiber (velvet) explosive emission cathodes have found widespread use in such varied applications as high power microwave generation [3], flash radiography sources [4], and pumping of eximer lasers [5]. In these applications the beam of electrons is generated by a cold cathode through explosive electron emission [6]. When a field exceeding ~16 kV/cm is applied to velvet patch, field enhancement occurs at the small radius tips of the dielectric fibers cause them to ionize [6]. This mechanism generates a layer of plasma from desorbed monolayers of gas along the cathode surface that expands axially and radially across the A-K gap via ohmic heating [7]. The plasma sheath provides a cloud of free electrons from which the electric field can extract a space-charge-limited flow. However, as the plasma expands into the A-K gap the impedance of the diode is reduced and with sufficient pulse lengths gap closure will occur [6]. For the pulse lengths utilized on the DARHT Axis I injector the effects of impedance collapse are negligible [7].

However, the formation of this plasma does play a role in the deformation of the emission surface [11].

Velvet has emerged as the dominant dielectric fiber material for a many cathode configurations [6, 8]. This is due to its low electric field threshold for plasma initiation, plasma uniformity, low cost, and low gap closure velocities compared to similar materials [7]. In addition this emission process does not require a cathode heater and it is able to operate at higher pressures than thermionic emission schemes [8]. As in the case of DARHT Axis 1, explosive emission type cathodes are the only option to support the 2kA current required for flash radiography.

However, despite these advantages high current planer geometry cathodes suffer from field depression in the center due to space charge effects from the beam [2,10]. This causes a non-uniform current density profile in the extracted beam to form, degrading the beam quality for the purpose of bremsstrahlung generation [4]. This effect has been investigated by Carl Ekdahl for the Axis I cathode with a flush geometry [2], showing a highly non-uniform current density profile in the transverse plane. It has been demonstrated that adding an inclination angle to the emission electrode with respect to the outer edge of the cathode can mitigate field depression [1]. Figure 1 shows 3 examples of such geometries taken from [1].

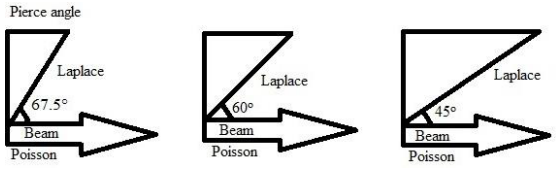

Figure 1: Electrode Inclination Geometries

To mitigate the effects of space charge depression, J.R. Pierce developed the pierce gun [13], which utilizes a curved cathode and incorporates an inclination angle of 67.5^{o} between the

emission surface (or beam profile) and the cathode shroud. This provides a focusing electrode geometry to generate a more uniform beam. The combined effect flattens the equipotential lines along the cathode surface that become distorted in the presence of space charge for a planer beam. An example of a thermionic type pierce gun design is shown in figure 2 [13].

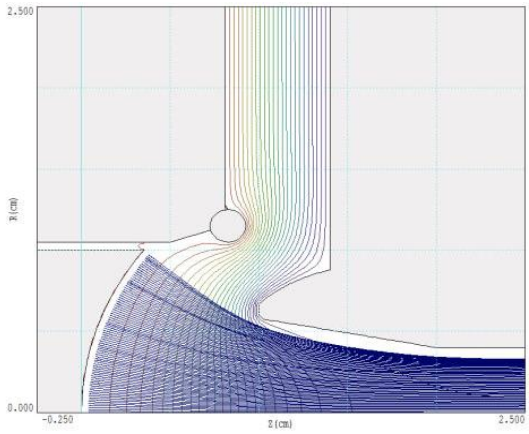

Figure 2: Example of Pierce Gun in Trak

The Pierce gun geometry has found wide use in a variety of applications [9], but it is not effective for intense highly relativistic electron beams. To this end, a number of focusing electrode angles are explored in this paper to semi-empirically determine a more effective cathode shroud geometry for the DARHT Axis I diode.

Background:

The DARHT Axis I injector tank shown in figure 3 has a 17.54 cm fixed A-K gap, a cathode shroud radius of ~30cm, and a tank wall radius of ~84 cm [7]. The cathode itself consists of a patch of black velvet ranging in size from 1.9-7cm with currents of 0.26-3 kA [2]. Axis I prime power delivers a 3.8 MV, 80ns pulse across the A-K gap during normal operation [7]. The cathode shroud has a 14 cm diameter space in the center for a cathode 'plug', allowing for the insertion

of different cathode geometries [3]. During normal operation the cathode plug is flat with a 2.5mm recess for the 5cm velvet cathode [2].

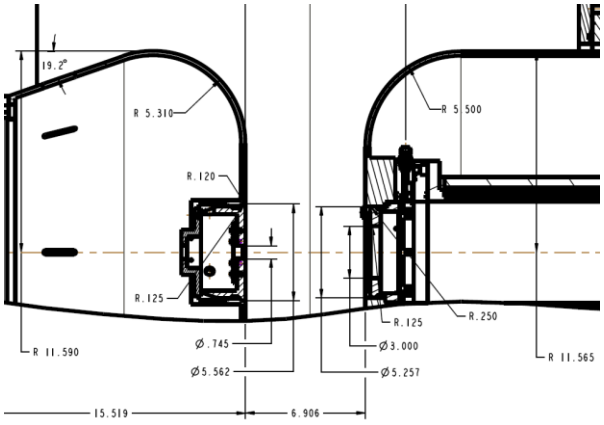

Figure 3: DARHT Axis I A-K gap (dimensions in inches)

During normal operation of DARHT Axis 1 a transformer is used to pulse-charge a 75Ω graded transmission line that delivers a nominal 3.8-4 MV, 100 ns pulse to the velvet cathode. Using the flat recessed geometry, the current extracted from a 2 inch velvet patch is between 1.5 and 1.8kA across the duration of the pulse (i.e. 2.2kΩ impedance) [10].

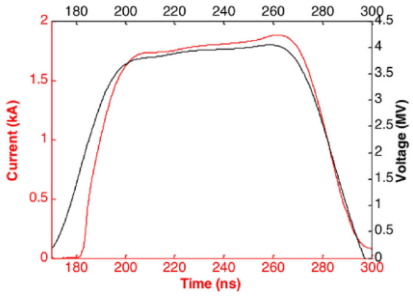

Figure 4: Nominal pulse delivered to 5cm cathode [10]

The simulations conducted are based on the 3.8 MV potential that exists on the cathode at approximately 190ns into the pulse of figure 4. The emission process takes place in the following steps: an electric field in excess of 10kV/cm is created causing an electron avalanche, monolayers of gas are desorbed from the velvet surface and ionized, and the cloud of ionized

gas provides a source of free electrons to initiate space-charge-limited current into the A-K gap [6]. The surface plasma then advances into the gap during the pulse, deforming the emission profile of the beam.

Method:

The simulations used in this investigation were conducted using the charged particle optics software Trak in conjunction with the field solutions programs in the TriComp suite created by Stan Humphries at Field Precision LLC [11]. Trak applies the triangular mesh finite element method [12] to solve single particle orbits in order to emit and transport them across user defined field geometries. The TriComp suite consists of the mesh generator MESH, and the electric and magnetic field solvers EStat and PerMag to generate field input files for the Trak software. Combining these programs provides a powerful tool for the simulation of electron and ion guns, electro-optical devices, and relativistic high-power beams.

A particle orbit solution is achieved by first generating a system geometry in the MESH drawing editor and defining the parameters of the mesh to be solved. An output mesh for the 2.5mm recessed diode geometry is displayed in figure 2, note the higher mesh densities in the regions of interest. Once the mesh is generated the electric field potentials can be solved in EStat. If there is a magnetic field component defined in the MESH geometry it can be solved in PerMag, but for the purpose of this investigation only electric field components were considered.

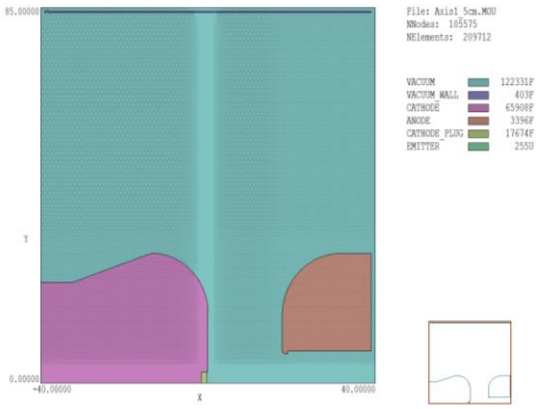

Figure 5: Example of MESH output for the simple recessed cathode geometry.

With the input mesh and fields generated, Trak can be used to calculate particle orbits and space charge effects in a number of different modes depending on the application. Because we are using 3.8MV across a 17.54cm A-K gap it is assumed that the beam is highly relativistic with $\gamma \gg 1$. Because of this we use the relativistic approximation 'RelBeam' mode in Trak. This mode includes both space charge effects on the electric field, as well as approximate the effects of beam generated magnetic fields.

Trak calculates these fields by filling field regions with a triangular mesh that conforms to the boundaries of each region. Mesh size is defined by the user and needs to be set to finer resolution in areas of intense field gradient or small radius boundaries. Once the mesh is established the potentials are calculated via the numerical form of Poisson's equation over the triangles that surround each vertex as seen in figure 6 [14]. Trak defines linear values such as permittivity and space charge as constant across the area of each triangular mesh element [14]. The vertex potentials at each point are then calculated iteratively by taking the weighted average of potentials at each of the neighboring points and the surrounding space-charge. A solution is converged on by iterative relaxation of the weighting factors.

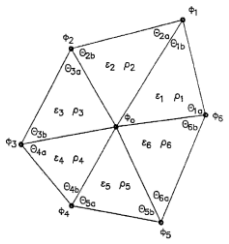

Figure 6: Example of finite-element mesh [14].

In both the relativistic and space charge limited modes Trak requires that an emission surface is defined and that there is short distance between it and the 'generation surface' [11]. This is done because the condition of space-charge-limited flow is such that the electron cloud generated in front of the emission surface causes a potential well, reducing the electric field on the surface of the cathode to zero [12], causing issues when modeling. Trak overcomes this difficulty by defining a generation surface that creates model particles representing groups of electrons that are nearby in phase-space and tracking their trajectories back to the cathode [11]. These particles are emitted at the temperature of the cathode and are assigned a transverse velocity $v_\perp$ approximating the Maxwell distribution via equation 1 [12].

$$f(v_\perp)dv_\perp = v_\perp\left(\frac{m_e}{kT_s}\right)\exp\left(-\frac{m_e v_\perp^2}{2kT_s}\right) \qquad (1)$$

The generation surface displacement was selected to be .01cm, and the number of emission segments was set to 6 for all simulations considered in this study. These values were empirically determined in previous work done by Carl Ekdahl [2].

For non-relativistic cases the force generated by self-magnetic field can be neglected, but as β approaches unity this effect becomes more significant [11]. The strong azimuthal self-magnetic field causes beam pinching due to the Lorentz force $F_r = v_z \times B_\theta$ [3]. The transverse

components of the electric and magnetic fields generated by a non-uniform, axially-symmetric beam can be determined from Poisson's equation and Ampere's law as follows:

$$E_r = -\frac{e}{2\pi\varepsilon_o r}\int_0^r 2\pi r' dr' n(r') \qquad (2)$$

$$B_\theta = -\frac{e\beta c\mu_o}{2\pi r}\int_0^r 2\pi r' dr' n(r') \qquad (3)$$

Where r is particle radius, z is longitudinal distance, $r' = \frac{dr}{dz}$, and n(r') is charge density. Then the force components due to the transverse electric and magnetic fields can be related by:

$$F_{B\theta} = -\beta^2 F_{Er} \qquad (4)$$

This pinching can be observed in the Trak results from the simple recessed electrode case in fig. 10. Figure 7 shows the comparison of a beamless electrostatic calculation (left) compared to the intense-space-charge modified case (right) when the beam is present. The deformation of equipotential lines near the axis can be clearly observed between the two cases.

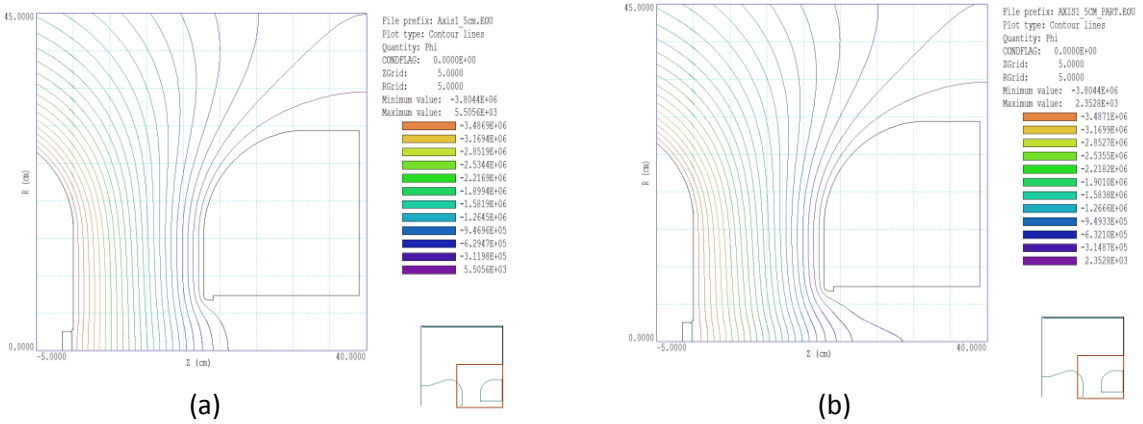

(a) (b)

Figure 7: (a) Electrostatic calculation from Estat without electron beam present, (b) Trak modified electric field with intense space charge beam present.

Results:

Track simulations were performed for 6 cathode geometries. For all geometries the emission surface was recessed by 2.5mm relative to the flat face of the cathode shroud, and the inclination angle between the emission surface and the surrounding cathode shroud was varied. As can be seen in figure 11 b for the 20 degree case, the edge of the cathode shroud and the emission surface have a 1mm radius fillet. This rounding was applied to all cathode geometries except the simple flat recessed case which has a 2mm fillet radius. In order to accurately represent this in the electric field calculations the mesh resolution is set to .1 mm in both the axial and radial dimensions for all cases in the region of the emission surface.

Trak simulations were performed for the current cathode shroud geometry and 5 additional cases where the cathode inclination angle was set to 20, 30, 45, 60, and 67.5 degrees. For each case the orbit profiles are shown in figures 10-15 (a & b), and current density profiles are shown in both a stacked (d) and waterfall (c) plot in order to demonstrate how the profile evolves as the beam travels in the axial direction. The current profiles were measured at regular axial positions in Trak, and analyzed in MATLAB. The current density 'J_z' is displayed in A/m^2 for all current density plots. In addition total current (figure 8) was measured for each case and a 'current density depression ratio' is represented as a figure of merit to judge the uniformity of each beam profile. Current density depression ratio was calculated by taking the ratio of the current density at the center of the beam (J_{ro}) to the maximum current density (J_{r_edge}) that occurs at the edge of the cathode at an axial location of z=1cm. In addition the normalized emittance (ε_n), measured in mm-mrad, is displayed for an additional figure of merit at an axial location of 30cm, which corresponds to a location neat the exit of the hollow anode.

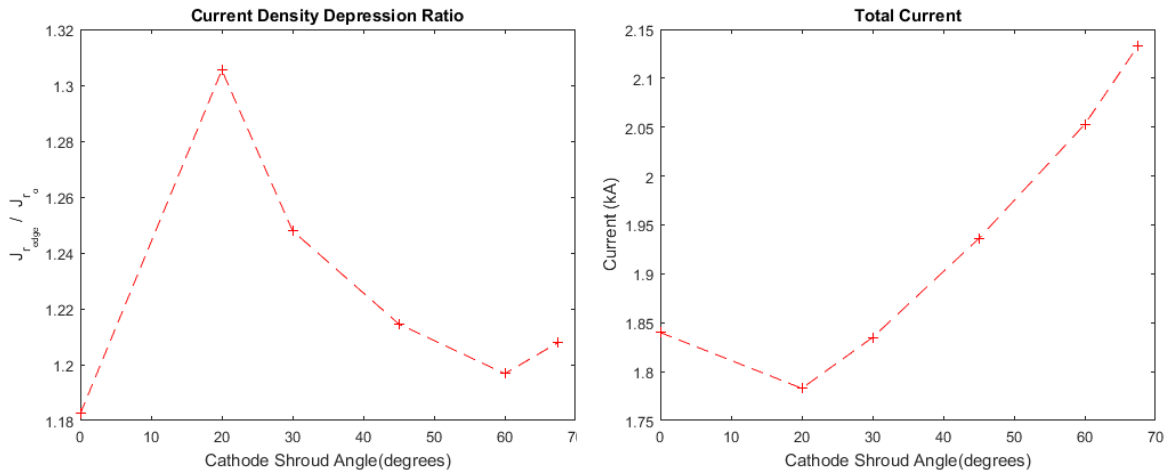

Figure 8: Current density depression ratio and total current versus angle

From figure 8 it can be observed that the simple recessed case exhibited the most uniform current densities but at the lowest current of 1.84kA. This total current seems to agree with previous work by Carl Ekdahl [2], in which the current for a 2mm recess was found to be 1.75kA and 2.25kA for the non-recessed case. It appears that the trend of increasing current with increasing cathode shroud angle also agrees with these previous results. Somewhat more surprising were the results for normalized emittance, the 30 degree case exhibited a large spike in emittance compared to other geometries. This value was initially considered to be an error, but the 30 degree case seems to follow the correct trend of total current increase. From a qualitative viewing of the results presented in figure 12 there does not appear to be anything overtly anomalous in the 30 degree case when compared to the results of the other cathode geometries.

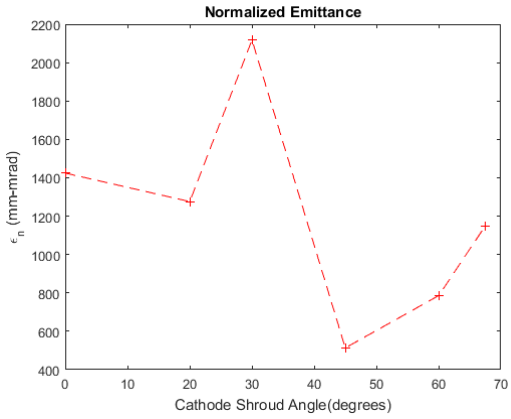

Figure 9: Normalized Emittances

Conclusion:

Simulations conducted with the Trak charged particle optics software showed close agreement with experimental data and provided insight into improved geometries for the DARHT Axis-I diode. Experimental results from DARHT Axis-I show a nominal current of 1.85kA [10] for a 2in cathode which strongly agrees with the Trak results for the simple recessed case. By changing the cathode shroud angle higher currents and lower emittances were achieved, showing promise for improved designs. However, despite the improved emittances of the 45, 60, and 67.5 degree cases the radial current uniformity was highest for the baseline recessed case currently employed on DARHT Axis-I [2]. More work will need to be done to mitigate this current non-uniformity in the future before a fieldable cathode design can be achieved. Of the selected geometries, the 45 degree case shows the best balance of cathode characteristics with the lowest emittance and modest improvements in total current while maintaining a relatively uniform current density. The 60 degree geometry also shows promise, warranting the investigation of additional smaller stepped angles in-between the 45 and 60 degree cases.

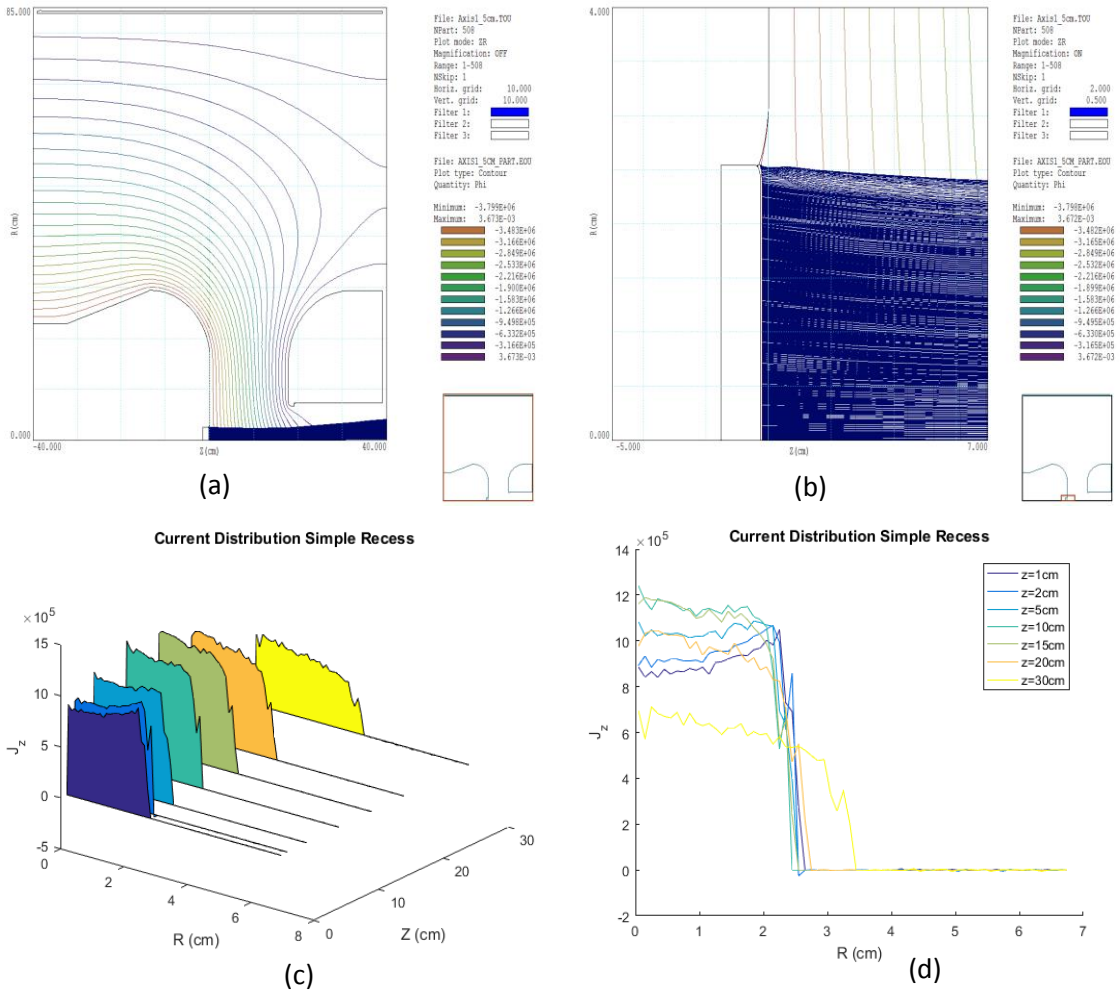

Figure 10: Simple 2.5mm recessed Cathode Geometry

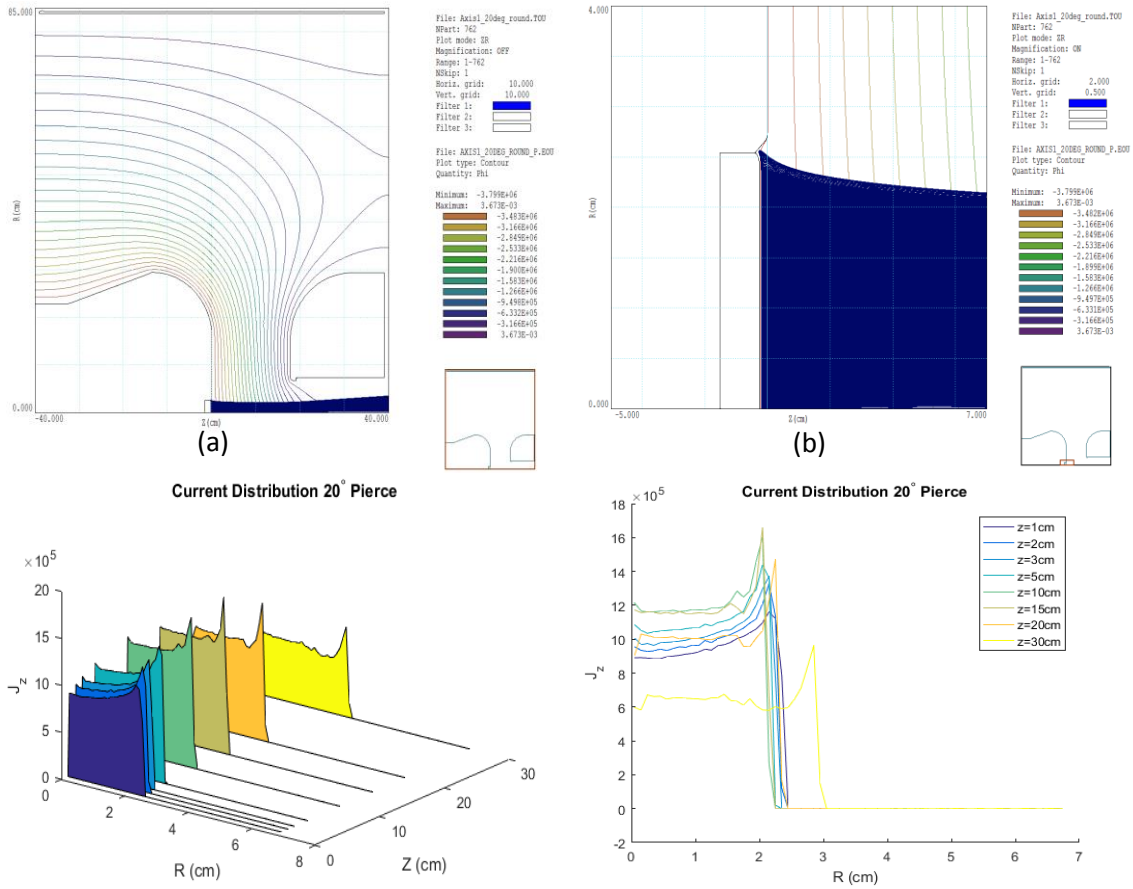

Figure 11: 20 Degree Inclination Angle

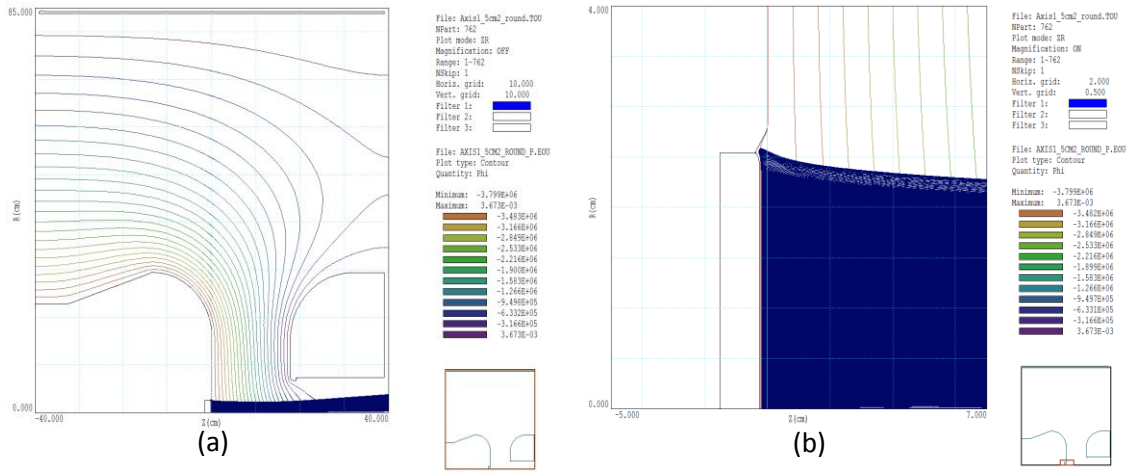

(a) (b)

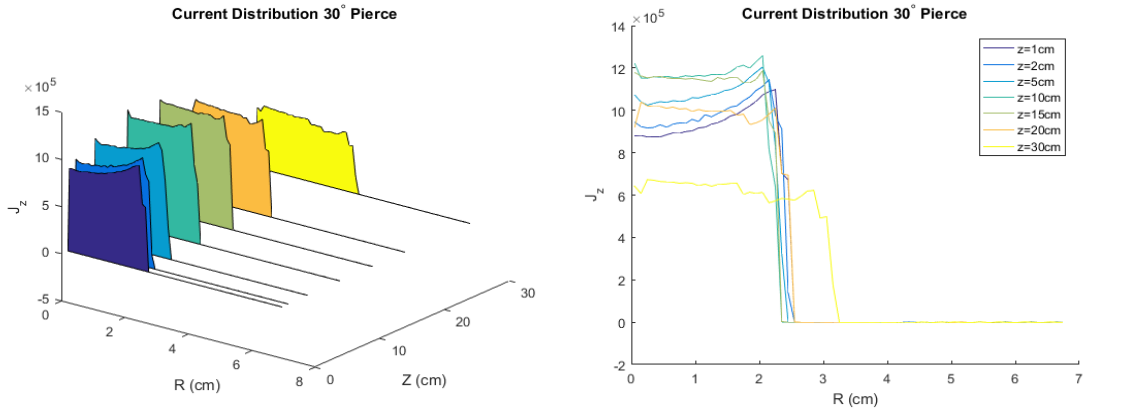

(c) (d)

Figure 12: 30 Degree Inclination Angle

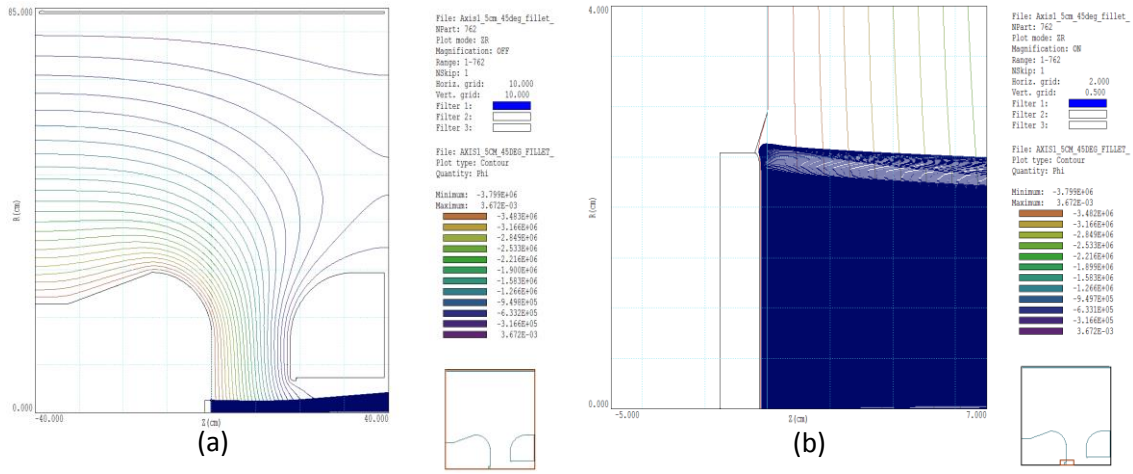

(a) (b)

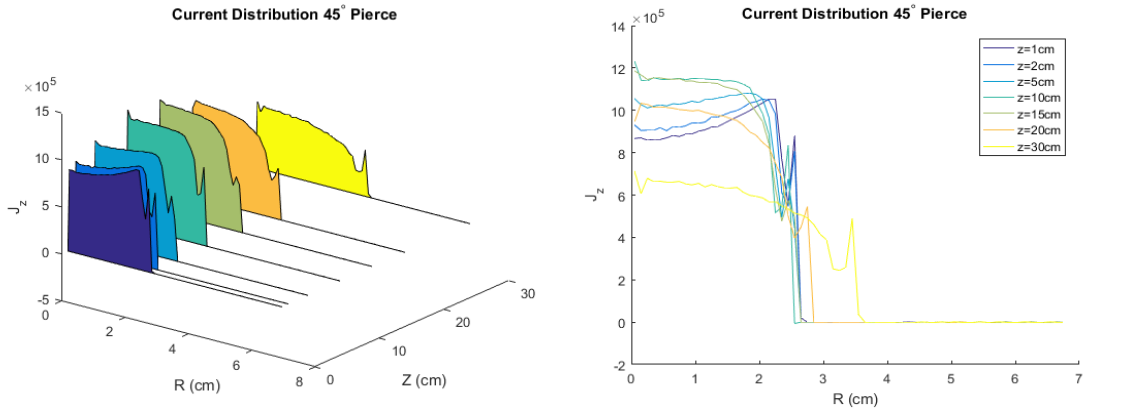

(c) (d)

Figure 13: 45 Degree Inclination Angle

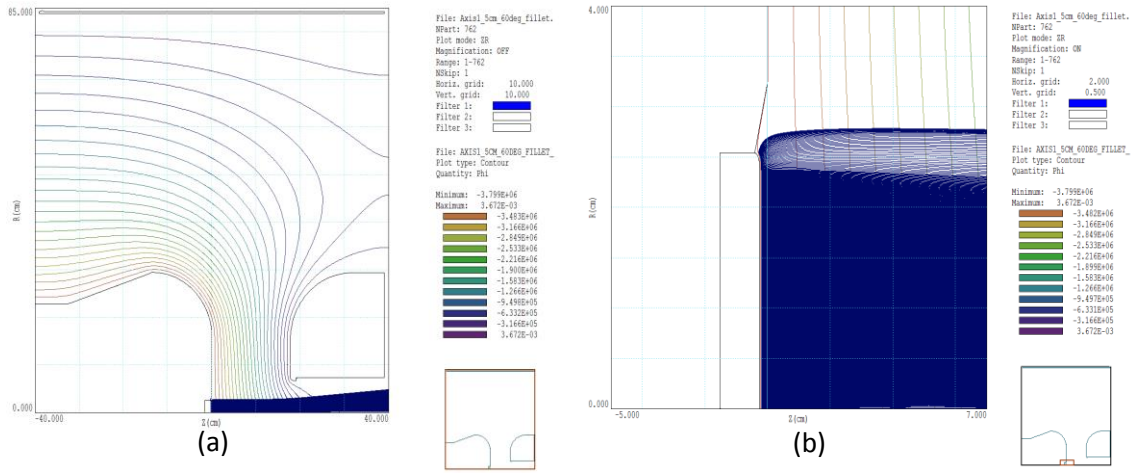

(a) (b)

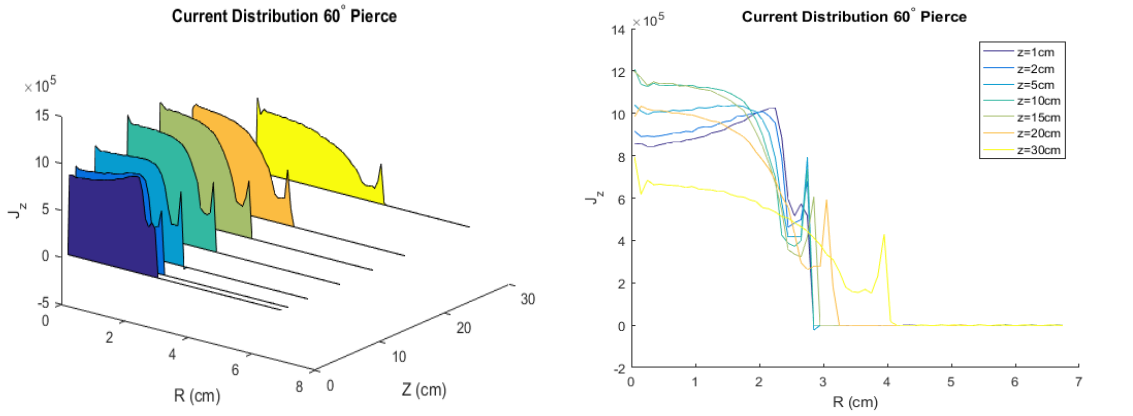

(c) (d)

Figure 14: 60 Degree Inclination Angle

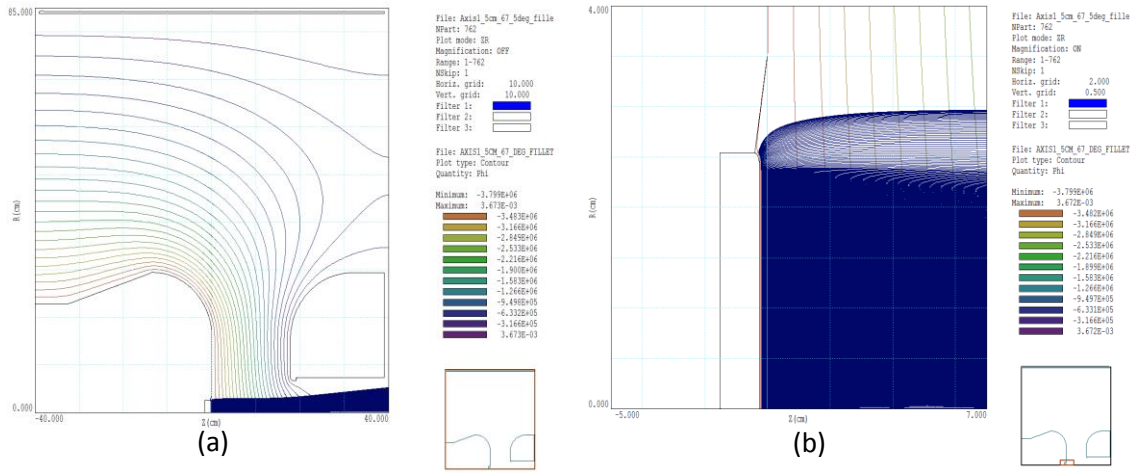

(a) (b)

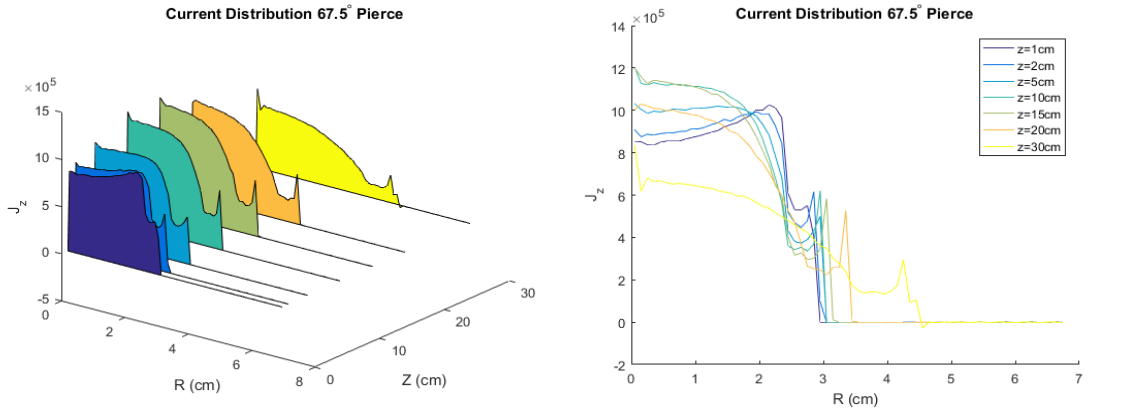

(c) (d)

Figure 15: 67.5 Degree Inclination Angle

References:

[1] M. Hoseinzade *et al* 2016 *Chinese Phys. C* 40 057003

[2] C.A. Ekdahl, "Axis-I Diode Simulations I: Standard 2-inch cathode," LA-UR-11-00206 (2011).

[3] J. Benford et al, "Microwave Fundamentals," in *High Power Microwaves, 3*th ed. Boca Raton, CRC Press, 2015, ch. *4*, sec. *6*, pp. *122–130.*

[4] J. E. Coleman, D. R. Welch, C. L. Miller, "Scattered hard X-ray and *γ*-ray generation from a chromatic electron beam," J. Appl. Phys., vol. 118, (2015).

[5] J. J. Ramirez and D. L. Cook, J. Appl. Phys. https://doi.org/JAPIAU51, 4602 (1980).

[6] R.B. Miller, "Mechanism of explosive emission for dielectric fiber (velvet) cathodes," J. Appl. Phys., vol. 84, (no. 7), pp. 3880- 3889, (1998).

[7] J. E. Coleman, D. C. Moir, C. A. Ekdahl, J. B. Johnson, B. T. McCuistian and M. T. Crawford, "Explosive emission and gap closure from a relativistic electron beam diode," *2013 19th IEEE Pulsed Power Conference (PPC)*, San Francisco, CA, 2013, pp. 1-6. doi: 10.1109/PPC.2013.6627454

[8] D. Shiffler, K. L. Cartwright, K. Lawrence, M. Ruebush, M. LaCour, K., Golby, and D. Zagar, Appl. Phys. Lett. 83, 428 (2003).

[9] A. El-Saftawy, Ashraf ; Elfalaky, Ahmed ; S. Ragheb, Magdi ; G. Zakhary, Safwat, " Investigation of Beam Performance Parameters in a Pierce-Type Electron Gun," Science and Technology, 11/1/2012, Vol.2(6), pp.191-197

[10] J. E. Coleman , D. C. Moir , M. T. Crawford , D. R. Welch , and D. T. Offermann, "Temporal response of surface flashover on a velvet cathode in a relativistic diode," Phys. Plasmas 22, 033508 (2015). https://doi.org/10.1063/1.4914851

[11] see: http://www.fieldp.com/manuals/trak.pdf

[12] Stanley Humphries Jr., "Trak – Charged particle tracking in electric and magnetic fields," in Computational Accelerator Physics, R. Ryne Ed., NewYork: American Institute of Physics, 1994, pp. 597-601.

[13] see: http://fieldp.com/myblog/2010/universal-high-flux-electron-gun-design/

[14] Stanley Humphries Jr., Numerical Modeling of Space-Charge-Limited Charged-Particle Emission on a Conformal Triangular Mesh, Journal of Computational Physics, Volume 125, Issue 2, 1996, Pages 488-497, ISSN 0021-9991, http://dx.doi.org/10.1006/jcph.1996.0110.
(http://www.sciencedirect.com/science/article/pii/S0021999196901102)